ELSEVIER

Journal of Nuclear Materials 255 (1998) 1–13

journal of nuclear materials

The effect of the cracking plane crystallographic orientation on the stress corrosion cracking process

Eugenia Ciocan [a,*], Margareta Ignat [b,1], Elena Gheorghiu [a]

[a] *Institute for Nuclear Research, PO Box 78, Pitesti 0300, Romania*
[b] *Faculty of Physics, University 'Al. I. Cuza', Iasi, Romania*

Received 6 June 1997; accepted 22 January 1998

Abstract

We have chosen from the literature a model which describes the SCC evolution considering three stages of the crack propagation: intergranular, transgranular and ductile rupture. We have verified the applicability of this model to describe the SCC failure of the CANDU type nuclear fuel and adapted it by considering the particular mechanical properties of the cladding, the actual value of the area of interest for SCC and by calculating the local concentration using the values of the iodine activities in the gap as predicted by an adequate fuel element computer code. We improved this overall model expressing the transgranular cracking threshold stress in terms of surface energy, crystallographic orientation of the fracture plane and of the fractional coverage with ZrI_4. The results of the calculations performed using this improved model confirmed the applicability of the model to describe the SCC failure of the CANDU type nuclear fuel.

1. Introduction

The most important factor affecting the integrity of nuclear fuel elements is the environmental assisted cracking (EAC). One of the EAC mechanisms is stress corrosion cracking (SCC). Stress corrosion cracking takes place when the irradiation embrittled cladding is subjected to high stresses during power ramps in the corrosive environment consisting of the fission products [1,2]. The defect mechanism under power ramping conditions was attributed to iodine induced stress corrosion cracking [3,4] due to the similarities between the fracture surface morphologies corresponding to the in-pile generated defects and to those produced by laboratory iodine induced SCC.

It has been demonstrated that iodine is liberated by γ radiolysis of solid CsI in a fuel rod under pressure and that the concentration of thus-liberated iodine is high enough to cause SCC of a Zircaloy cladding [5]. Iodine can react with the metal of the cladding to form zirconium iodide, considered to be representative of corrosive or embrittling species present in a fuel rod [6]. The corrosive effect of iodine and zirconium iodides is the weakening of the Zr–Zr bond at the crack tip. The iodine induced embrittlement of Zr may be considered [3,7] analogous to the grain boundary embrittlement or temper embrittlement of steels (materials fracture as a consequence of cohesion lowering along grain boundaries due to elemental segregation [8]). The common cause of these phenomena is the reduction of surface energy which promotes the propagation of Griffith cracks [7]. This phenomenon has been intensively studied [9–11] due to its importance in describing the chemically assisted fracture.

* Corresponding author. Tel.: +40-48 213 400 (extension 140); fax: +40-13 125 896; e-mail: eciocan@cc.nuclear.ro.
[1] E-mail: emignat@uaic.ro.

0022-3115/98/$19.00
PII S0022-3115(98)00023-3

Crack initiation is considered to be the controlling step in SCC of the cladding tubes [12]. Attempts have been made to describe the crack initiation either by starting from experimental work and establishing the log-normal distribution of the initial crack lengths [4] or by trying to explain it by creep mechanisms [7]. A detailed model was developed in paper [3], describing the crack initiation by diffusion-controlled cavitation of the grain boundary including the effects of metal embrittlement by iodine species. The crack initiation stage, associated with void nucleation, is generally recognised to dominate the failure times for initially undamaged materials [3]. Other authors associated the crack initiation sites in the fuel element cladding with the pre-existing (chemical and mechanical) defects [13,14]. It is possible that the internal surface of the fuel element cladding contain chemical and mechanical fabrication defects having radial dimensions up to 10% of the cladding thickness. These defects can be considered incipient cracks.

The crack propagation is caused by the high stresses appearing during the rapid increases of the fuel linear power (power ramps) that accompany the refuelling operation in CANDU reactors. The stresses due to the expansion of the fuel pellets are considered to be concentrated in the cladding zones corresponding to pellet–pellet interfaces. The stress–strain curve of the irradiated material can be used to express the mechanical properties of the cladding and it contains implicitly the irradiation embrittlement effect.

The fuel cladding having the internal surface coated with a graphite layer is characterised by a lower failure rate through the SCC mechanism than the fuel cladding without graphite coating. The role of the graphite layer in reducing the corrosive effect of the iodine and its compounds is not entirely clarified. It has been shown [15] that stable Zr_xI_yC and $CsZr_xI_yC$ can be formed in samples of oxidised CANLUB coated Zy-4 cladding exposed to I_2 and CsI, respectively, at 320°C. The formation of these compounds should reduce the SCC process because the compounds are binding the corrosive reactants (such as ZrI_4 and CsI). The corrosive species can also be retained in the graphite layer by adsorption and absorption [2,16]. It was possible to express the amount of fission products reacted/absorbed/adsorbed by the graphite per unit mass of graphite [2] and consequently to account for the reduction of the iodine coverage at the inner surface of the cladding.

There are two possibilities to describe the cladding SCC failure process. The first one evaluates the SCC failure probability during in reactor operation as an empirical function of the operation parameters (burnup, linear power, and linear power increase during a power ramp) named fuelogram [17]. These probabilities have been established using the experimental data available from in reactor operation of the fuel elements and are used to evaluate the threshold values of the operation parameters for which, at the considered burnup, the fuel elements are not affected by the SCC failure process during power ramps. A second possibility to describe SCC failure process is modelling the evolution of the stress corrosion crack in order to obtain a better understanding of the process. The development of models to describe the fuel cladding SCC phenomenon is also a necessary step to evaluate the failure thresholds for the parameters describing the fuel element behaviour (local stress in the cladding, local iodine concentration) [2,18].

In this paper we have tried to put together several models found in literature in order to express the dependence of the time to SCC failure on the crystallographic orientation of the cracking plane. In Section 2.1 we describe the phenomenological model starting from which we developed a program to describe the stress corrosion crack propagation in the cladding of the CANDU type fuel element. In Section 2.2 we describe the improvements we have brought to this model to reach our goal. In Section 2.2.1 we describe how the criterion of transgranular cracking can be written in terms of the surface energy and of the plastic work. In Section 2.2.2 we present the model used to express the plastic work as a function of the surface energy. In Section 2.2.3 the dependence of the surface energy on the crystallographic orientation of the cracking plane and on the iodine fractional coverage is described. The results we obtained are presented in Section 3.

2. The model

2.1. Phenomenological model for the iodine stress corrosion crack propagation

We have selected from the literature [13] as a model to describe the cladding stress corrosion cracking and adapted it [19] to describe the stress corrosion cracking for the CANDU type fuel element cladding.

The assumptions of the model are summarised below [13] and completed with our adaptations.

(I1)

(a) The mechanical and chemical flaws in the cladding wall are supposed to be sites where stress corrosion cracks can be initiated and they can be considered as initial cracks.

(b) Only the areas on the internal surface of the cladding adjacent to pellet–pellet interfaces are of interest for SCC. This fact is supported by the experimental observation [20] which showed the concentration of the fission products on the internal surface of the cladding near the pellet–pellet interfaces. On the other hand it is known that important stress concentrations take place in the cladding in the vicinity of the pellet–pellet interfaces and at the end caps. Given N the number of nuclear

fuel pellets in the considered fuel element, there are $N+1$ such surfaces of interest for the SCC phenomenon. The total area of the surface of interest for SCC, A_s, is given by

$$A_s = \pi\, dl(N+1), \tag{1}$$

where: d is the internal diameter of the cladding; l is the width of the annular area in the cladding where the fission products are supposed to concentrate; in our calculations we considered $l = 10^{-3}$ m.

(c) The distribution of the initial cracks is supposed to be Weibull type [13]:

$$\phi(c_0) = 1 - \exp\left[-kA_s\left(1/\sqrt{c_0}\right)^p\right], \tag{2}$$

where k and p are constants as defined in Ref. [13]; c_0 is the initial crack length; A_s is the surface area of interest for SCC of the fuel element given by Eq. (1).

(I2)

(a) To describe the evolution of the stress corrosion crack, the transversal section of the cladding is assumed to consist in a certain number of radial elements (annuli). We considered these annuli of width equal to the initial crack length.

(b) The local iodine concentration can be calculated using the equation

$$c = \frac{1}{A_s} u \sum_{i=1}^{4} A_i \frac{\Lambda_i}{\lambda_i}, \tag{3}$$

where: A_s is defined by Eq. (2); u is the atomic mass unity; Λ_i is the activity of the ith iodine isotope ($i = \overline{1,4}$: ^{131}I, ^{132}I, ^{133}I, ^{135}I) as it has been calculated with a computer code which describes the fuel element behaviour; λ_i is the radioactive constant of the ith iodine isotope; A_i is the atomic mass of the ith iodine isotope.

(c) According to the model proposed in Ref. [13], iodine penetration into the Zircaloy is assumed to be a diffusionlike process and surface diffusion and/or adsorption is rate controlling. As a consequence, iodine penetration is permitted only in the first unfailed element of the cladding and the rate of increase of the iodine concentration, I, at the first unfailed element is given by the equation

$$\frac{\mathrm{d}I}{\mathrm{d}t} = \frac{I_3}{w}\exp\left(-\frac{Q}{RT}\right)\left[I_{\mathrm{eff}}\exp\left(-\frac{k_5}{\varepsilon^{k_6}}\right) - I\right], \tag{4}$$

where: the constants I_3, I_{eff}, k_5, k_6 and the activation energy for iodine diffusion, Q, were given in Ref. [13]; w is the width of the fuel cladding; T is the absolute temperature of the internal surface of the cladding and ε is the local strain in the first unfailed element. The surface reactions have been neglected in this first approximation. The model described in the paper [13] that we have chosen [19] permits further improvements in the evaluation of the iodine concentration by considering in the left hand side of the Eq. (4) terms which account explicitly for the surface reactions in which iodine is generated or lost.

(I3)

(a) The stress, σ_i, for each element is assumed to have the following expression [13]:

$$\sigma_i = \sigma_i^{\mathrm{u}} + \sigma_i^{\mathrm{tr}}; \qquad i = \overline{1,n}, \tag{5}$$

where: σ_i^{tr} describes the material behaviour during uniaxial stress and can be evaluated using the stress–strain curve, σ_i^{tr} is a term which accounts for plastic constraint and stress triaxiality at the crack tip and its expression is considered to be given by

$$\sigma_i^{\mathrm{u}} = 2\sigma_y\left[1 - \exp(-k_3 B)\right]\left(\frac{\nu_i - \nu_n}{\nu_{\mathrm{ct}} - \nu_n}\right)^2, \qquad i = \overline{1,n}, \tag{5'}$$

where: k_3 is a constant [13] and the strain in the ith annular element, ν_{i} is the radial distance from the ith annulus to the annulus situated at equal distances from the external and the internal surfaces; ct is the index corresponding to the element where the crack tip is placed and B is defined in connection with Eq. (6).

The strain, ε_i, for each element is given by Ref. [13]:

$$\varepsilon_i = A + B\left[\exp(-k_2 \nu_i) - 1\right], \qquad i = \overline{1,n}, \tag{6}$$

where A, B are the degrees of freedom for Eq. (6) and k_2 is a constant [13].

(b) Mechanical equilibrium conditions are considered to be fulfilled:

$$\sigma_{\mathrm{h}} = \frac{\sum_{i=n_{\mathrm{u}}}^{n} \sigma_i \Delta A_i}{\sum_{i=1}^{n} \Delta A_i}; \tag{7}$$

$$(M)_{v=0} = 0 = \sum_{i=n_u}^{n} \sigma_i \Delta A_i v_i; \tag{8}$$

where: σ_h is the overall hoop stress in the cladding, $(M)_{v=0}$ is the resultant moment about the point with $v=0$, ΔA_i is the area of the ith element; n_u is the index of the first unfailed element, n is the total number of radial elements. Based on experimental observations the model supposes that the corrosion crack propagation process has three stages: intergranular cracking, transgranular cracking and ductile rupture. The local failure criteria have been determined using experimental data [13]: intergranular cracking criterion

$$I \geq I_{IG} = 10^{-6}\,\mathrm{g/cm^2}, \tag{9}$$

where I is the local iodine concentration;transgranular cracking criterion

$$\sigma_{n_u} \geq \sigma_{0,c+f}, \tag{10}$$

$$1 \geq I_{TG} = I_{IG}\left(\frac{\sigma_{0,c+f}}{\sigma}\right); \tag{11}$$

ductile rupture criterion

$$\varepsilon_{n_u} \geq \varepsilon_R = \varepsilon_R^u\left[\frac{1}{3} + \frac{2}{3}\exp(-k_3 B)\right], \tag{12}$$

where: $\sigma_{0,c+f}$ is the stress limit for SCC; ε_R^u, k_3 and B are constants [13]; σ_{n_u} and ε_{n_u} are the local stress and strain in the first unfailed element, respectively.

With these assumptions and criteria, the problem of describing the evolution of the stress corrosion crack in the fuel element cladding becomes one of solving a $(2n+2)$ equation system (Eqs. (5)–(8)) with $(2n+2)$ unknown quantities (A, B, ε_i, $i=\overline{1,n}$, σ_i, $i=\overline{1,n}$). Starting from this model we have developed a computer program [19]. This program evaluates the time to SCC failure for a given power history containing a power ramp.

We have chosen the overall model described in Ref. [13] because it could be adapted to describe the SCC behaviour of CANDU type fuel elements through the use of the particular values for the area A_s corresponding to the surface of interest for SCC, for the iodine concentration at the surfaces of interest for SCC (evaluated starting from the values of the iodine isotope activities in the gap predicted by a fuel code) and for the temperature of the inner surface of the cladding; the model has also permitted the consideration of the adequate stress–strain curve. On the other hand, we have chosen the model described in Ref. [13] because it can be used in connection with a computer code which does not perform finite element analysis to evaluate the stress in the cladding but computes the overall hoop stress in the cladding, σ_h.

2.2. Model to describe the dependence of the SCC process on the crystallographic orientation of the cracking plane and on the iodine fractional coverage

We were interested in expressing quantitatively the dependence of the SCC time to failure on the crystallographic orientation of the cracking plane. For this reason, we have tried to improve the overall model described in Ref. [13] expressing the transgranular failure criterion in terms of surface energy. Then we expressed the surface energy as a function of the Miller indices of the crystallographic plane where the atomic bond breaking takes place.

2.2.1. The dependence of the stress threshold for transgranular crack propagation on the surface energy

The threshold stress for the transgranular propagation of the stress corrosion crack was deduced [13] from K_{ISCC} data obtained from unirradiated Zircaloy with typical basal pole texture (the peak density of the basal poles at $\sim 30°$ to the radial direction). We can express this threshold stress in thermodynamic terms, considering the crack propagation to be an equilibrium process [21,22]. We assume that the crack is 'infinitely' sharp and that it propagates in the mode I (opening mode).

When the cladding material is considered to be elastic, the thermodynamic criterion for the crack propagation is [22]

$$\sigma_{n_u} = \sigma^{\max} \geq \sigma_{0,c+f} = 2\sqrt{\frac{c}{\rho}}\sqrt{\frac{2E\gamma_0}{\pi c}} = 2\sqrt{\frac{2E\gamma_0}{\pi\rho}}, \tag{13}$$

where: E is Young's modulus; the stress concentration factor for an 'infinitely' sharp crack, $(\sigma^{\max})/(\sigma)$, where σ and $\sigma^{\max}$ are the applied and the local stress corresponding to the crack extension, was expressed [22] as $2\sqrt{(c/\rho)}$, c being the crack length and ρ being the radius of curvature at the crack tip; γ_0 is the surface energy. The surface energy is defined [22] as the work done in creating a new surface area by breaking of atomic bonds.

When the cladding material is considered to be a brittle deformable one, a realistic fracture theory must take into account the ideal fracture work and the plastic work due to the dislocation emission in front of the crack, γ_p [23]. As a result, the transgranular cracking criterion for the local stress becomes

$$\sigma_{n_u} = \sigma^{\max} \geq \sigma_{0,c+f} = 2\sqrt{\frac{c}{\rho}}\sqrt{\frac{E(2\gamma_0+\gamma_p)}{\pi c}} = 2\sqrt{\frac{E(2\gamma_0+\gamma_p)}{\pi\rho}}\,. \tag{14}$$

Although the representation of the mechanical work of cracking as a sum between the plastical work γ_p and the elastical work, γ_0 is controversial [24], we considered it as a first approximation step. The aim of this paper was to show the possibility of quantitatively expressing the dependence of the SCC time to failure on the orientation of the cracking plane and we consider that this approximation would not affect drastically the conclusions of our work. Considering in Eq. (13) the average values for E and γ_0 in Zircaloy-4, we could determine from the value of $\sigma_{0,c+f}$ used in Ref. [13] the order of magnitude of the average curvature radius at the crack tip as being 10^{-5} m.

2.2.2. The dependence of the plastic work on the surface energy

We could evaluate the dependence of the plastic work of fracture, $w_p|_{\text{fracture}} = \gamma_p$, on the ideal work of fracture, γ, using the model presented in Ref. [23]—a microscopic theory of deformable solids fracture which establishes the relation between the fracture ideal work and the plastic work. The model assumptions are briefly pointed out below.

(I1) The static analysis can be applied to the dynamic process of crack propagation.

(I2) The dislocation emission at the crack tip and the bond stretching are simultaneous processes.

(I3) Plastic work is caused by the network resistance to the dislocation movement only and the contribution of the dislocation nucleation can be neglected.

(I4) Dislocations emitted at the crack tip are in the crack plane so that a Dudgale–Bilby–Cottrell–Swinden (DBCS) model can be applied.

(I5) The speed of the dislocations under stress depends on a certain constant power, n, of the local stress.

(I6) Only the bond between the first atom pair (nearest to the microcrack tip) is implied in the cracking process and the restoring force is harmonic.

(I7) The extent of the plastic zone, s, is much less than the crack length, c.

We shall shortly discuss here the applicability of the model described in Ref. [23] to Zircaloy-4. In Ref. [23] it is stated that a microcrack must be nucleated ahead a notch or a precrack, for example at a carbide or another hard inclusion in steel. For Zircaloy-4, in the overall model [13] we adopted, cracks can be initiated at sites of chemical inhomogeneity at the inner surface; it is considered that when local iodine concentration is greater or equal to I_{IG} intergranular propagation of crack takes place. In this paper we consider that the intergranular cracking produces the fresh microcrack starting from which the Griffith type fracture will proceed.

In Ref. [23] a DBCS model is used for the dislocations emitted at the crack tip. The plastic work, w_p, produced by dislocations during the time t is expressed as

$$w_p = \frac{3\pi G}{8}\left[\frac{\Phi_0(1-\upsilon)^{n-1}(n+1)^2}{2^{3n+1}}\left(\frac{K}{G}\right)^{4n} t^2\right]^{\frac{1}{n+1}}, \tag{15}$$

where: G is the shear modulus; K is the stress intensity factor; t is the time at which we evaluate the plastic work; υ is Poisson ratio; $\Phi_0 = g\boldsymbol{b}v_0$; $\boldsymbol{b}$ is the Burgers vector; v_0 is an empirical parameter, g^{-1} is the linear spacing of the emitted dislocations or the distance over which any emitted dislocation has to move away from the microcrack tip before the next dislocation can be emitted; n is a constant as defined in assumption (I5) [23]. Φ_0 and n are considered adjustable parameters of the model.

To evaluate the plastic work per unit length of the virtual microcrack extension, we are interested now in evaluating the time corresponding to bond breaking. Considering assumption (I6), if $\ddot{y}$ is the coordinate perpendicular to the plane of the microcrack, that is the direction of the bond stretching, the equation of motion of the atom pair is

$$m\ddot{y} = -\kappa y + b^2\tau(t), \tag{16}$$

where: m is the mass of one atom, κ is the elastic constant of the bond; b^2 is the area per atom and τ denotes the local stress. It is assumed that the restoring force vanishes when a bond is stretched through a displacement δ. When the surface energy γ is small or the stress intensity factor, K, is large, Eq. (16) can be approximated by

$$\ddot{y} = \frac{b^2}{m}\tau(t). \tag{17}$$

Using the model DBCS, the expression for the time at which the bond breaks, t_b, was determined in Ref. [23] as being

$$t_b = \left[\frac{n(2n+1)\delta}{\beta(n+1)^2}\right]^{\frac{n+1}{n+2}} \left(\frac{K}{G}\right)^{-\frac{2}{2n+1}}, \tag{18}$$

where

$$\beta = \frac{b^2}{m} G \left[\frac{1-\upsilon}{2\Phi_0(n+1)}\right]^{\frac{1}{n+1}}. \tag{19}$$

Introducing t from Eq. (18) in Eq. (15), we obtain the correct expression for the plastic work as

$$w_p = \frac{3\pi}{8} 2^{\frac{3(2n-1)}{2n+1}} (1-\upsilon)^{\frac{2n-3}{2n+1}} \left[\frac{n(2n+1)m\delta\Phi_0^2 G^{\frac{2n-1}{2}}}{2b^2}\right]^{\frac{2}{2n+1}} \left(\frac{K}{G}\right)^{\frac{4(2n-1)}{2n+1}}. \tag{20}$$

The thermodynamic criterion for unstable microcrack extension for deformable solids can be written as [23]

$$E = -\frac{K^2}{2G}(1-\upsilon) + 2\gamma + w_p(\gamma, K) \le 0, \tag{21}$$

where E is the total energy of the system. Taking into account Eq. (20), the condition given in Eq. (21) can be written as

$$U_{EN} = -K_{EN}^2 \frac{(1-\upsilon)}{2} + 2p + rK_{EN}^{\frac{4(2n-1)}{2n+1}} \le 0, \tag{22}$$

where we used the following notations:

$$\begin{cases} U_{EN} = \dfrac{E}{Gb} \\ K_{EN} = \dfrac{K}{G\sqrt{b}} \\ p = \dfrac{\gamma}{Gb} \\ r = \dfrac{3\pi}{8} 2^{\frac{3(2n-1)}{2n+1}} (1-\upsilon)^{\frac{2n-3}{2n+1}} \left[\dfrac{n(2n+1)m\delta b^{(2n-7)/2}}{2G}\right]^{2/(2n+1)} \end{cases}. \tag{23}$$

The equality in relations (Eq. (21)) and (Eq. (22)) corresponds to the equilibrium of the crack. We could calculate K_{EN}, and consequently K, by numerically solving Eq. (22′):

$$-K_{EN}^2 \frac{(1-\upsilon)}{2} + 2p + rK_{EN}^{\frac{4(2n-1)}{2n+1}} = 0, \tag{22′}$$

for any given value of the surface energy, γ. With this value of K corresponding to the fracture, K_G, and taking into account the condition of the microcrack equilibrium as contained in Eq. (21) we could express the value of $w_p|_{\text{fracture}} = \gamma_p$ for the considered value of γ.

2.2.3. The dependence of the surface energy on the crystallographic orientation of the cracking plane and on the iodine fractional coverage

We suppose that all the iodine species considered active in the SCC process react with Zircaloy and produce ZrI_4. Following the assumption of Williford [3], we neglected the formation of ZrI_x ($x < 4$) species. The rate at which ZrI_4 is produced by Zircaloy–iodine reaction has been described using a simple first-order chemical rate reaction [6]:

$$I_R = I_0(1 - e^{-Kt}), \tag{24}$$

where I_R is the concentration of iodine which reacted with the Zircaloy, I_0 is the concentration of free iodine initially at the crack tip, t is the time and K is the reaction rate constant. In paper [6], K is considered to be given by

$$K = \frac{kT}{h} e^{-Q/RT}, \tag{25}$$

where k is Boltzmann's constant, h is Planck's constant, T is the absolute temperature and $Q = 1.16 \times 10^5$ J/mol K is the activation energy [6].

We consider here that all iodine species react with Zircaloy following the rate reaction expressed by Eq. (24), with the same reaction rate constant given by Eq. (25). Further improvements can be made in the model considering the real values of the sticking coefficients for each iodine isotope in order to express the chemical reaction rate constant corresponding to each iodine isotope more precisely.

The modified Langmuir isotherm [3,6,7] was used to represent the adsorption of the assumed embrittling agent onto the metal surface:

$$\theta = \frac{p_r}{1 + p_r}, \qquad \text{with } p_r = \log \frac{P}{p_c}, \tag{26}$$

where θ is the fractional surface coverage, p is the ZrI_4 pressure, p_c is the critical pressure representing the initiation of the observable SCC effects; $p_c = 10^{-2}$ Pa [6].

The ZrI_4 is assumed to embrittle Zy by reducing its surface energy [3,7]:

$$\gamma_s = \gamma_0 + \Delta\gamma, \qquad \Delta\gamma < 0, \tag{27}$$

where $\gamma_0 \cong 1$ J/m^2 is the initial surface energy of the Zircaloy in the unembrittled state; $\Delta\gamma$ was calculated [3] using Gibbs equation as follows:

$$\Delta\gamma = -\frac{\theta S}{A_N} RT \mathrm{d}(\ln P), \tag{28}$$

where S is the surface atom density, A_N is Avogadro' s number and R is the ideal gas constant. The logarithmic pressure differential, d(ln P), was evaluated [3] taking into account that below p_c SCC effects are negligible and thus Eq. (28) took the form

$$\Delta\gamma = -\frac{\theta S}{A_N} RT \ln(p/p_c), \tag{29}$$

where $\ln(p/p_c)$ can be expressed from Eq. (26); thus

$$\Delta\gamma = -\frac{S}{A_N} RT \frac{\theta^2}{1-\theta} \ln 10. \tag{30}$$

Hwang and Han [7] expressed the surface atom density S in Eq. (30) as the inverse of the area S_{hkil} of a primitive unit mesh surface and considered the following relation giving S_{hkil} as a function of the Miller indices, i, j, k and l in the hcp crystal:

$$S_{hkil} = \frac{1}{2} a^2 \left[4 \left(\frac{c}{a} \right)^2 (h^2 + hk + k^2) + 31^2 \right]^{1/2}. \tag{31}$$

This was the way to express the reduction of surface energy as a function of the Miller indices of the considered surface [7]:

$$\Delta\gamma_{hkil} = \frac{1}{S_{hkil} N_A} RT \frac{\theta^2}{1-\theta} \ln 10. \tag{32}$$

Eq. (27) could be written as [7]

$$\gamma_s = \gamma_{0,hkil} - \Delta\gamma_{hkil} \tag{33}$$

in order to emphasise the dependence of the surface energy on the Miller indices of the considered surface.

The surface energies at 0 K are given [7] as follows:

$$\gamma_{0,hkil} = q\gamma_b; \tag{34}$$

where γ_b is the energy of the basal plane which serves as a reference value, and q was considered to be [7]

$$q = \begin{cases} \dfrac{4h + 4k + 3\zeta l}{3\zeta\sqrt{\dfrac{4}{3}\left(\dfrac{c}{a}\right)^2 (h^2 + hk + k^2) + l^2}} & \text{region limited by } (0001)(11\bar{2}2)(10\bar{1}1) \\ \dfrac{4h + 4k + (2h + 2k + l)\zeta}{3\zeta\sqrt{\dfrac{4}{3}\left(\dfrac{c}{a}\right)^2 (h^2 + hk + k^2) + l^2}} & \text{region limited by } (11\bar{2}2)(10\bar{1}1)(11\bar{2}0) \end{cases}, \tag{35}$$

where ζ was evaluated [7] as 1.1412 for zirconium.

3. Computational results

3.1. The dependence of the time to failure on the applied stress

We have studied the applicability of the model presented in Ref. [13], with adaptations shown in Section 2.1 for local concentration calculation and for the stress–strain curve, in describing the SCC behaviour of the CANDU type fuel.

Primarily, we verified the dependence of the time to SCC failure, t_{fSCC}, on the applied stress considering several stress–strain curves. The results obtained for the irradiated cladding at 598 K and 617 K are presented in Figs. 1 and 2 comparatively with the results obtained by the authors of the model, noted JNM_99. The stress–strain curves used in performing calculations were: (1) obtained in INR in tensile tests on irradiated Zircaloy-4 cladding samples at 573 K [25]; the corresponding results were noted INR_ax; (2) obtained in INR in burst tests on irradiated Zircaloy-4 cladding samples at 573 K [25]; the corresponding results were noted INR_burst; (3) found in the literature [26] and obtained by straining in iodine and argon environment at 629 K samples obtained by tangential prelevation from claddings; the corresponding results have been noted JNM_199(tg_I) and JNM_199(tg_Ar).

The dependencies evaluated using our program follow those determined by the authors of the model. We consider that the differences observed are caused by the different stress–strain curves we have used. For further calculations with our model, we selected the stress–strain curves determined in the burst tests performed in INR on irradiated Zircaloy-4.

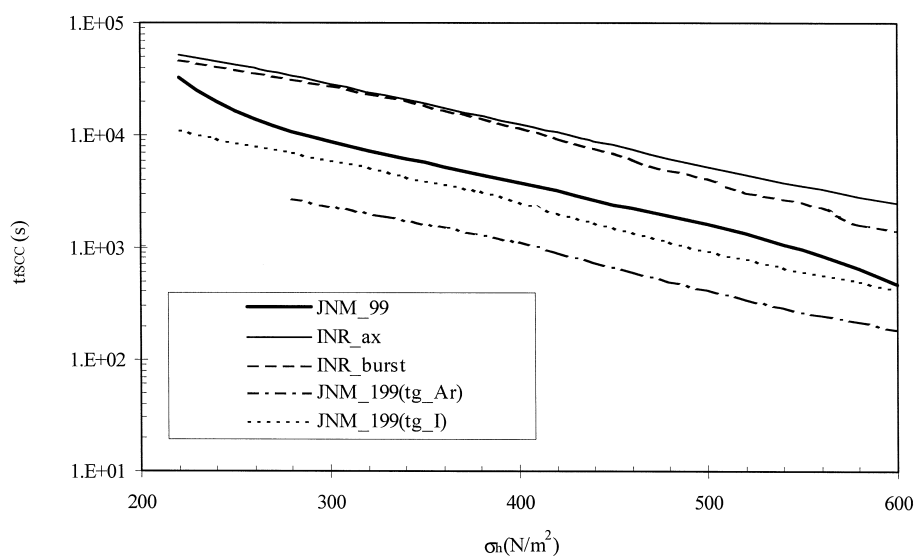

Fig. 1. The dependence of the SCC time to failure of the cladding, t_{fSCC}, on the macroscopic hoop stress, σ_h; $T = 598$ K; irradiated material.

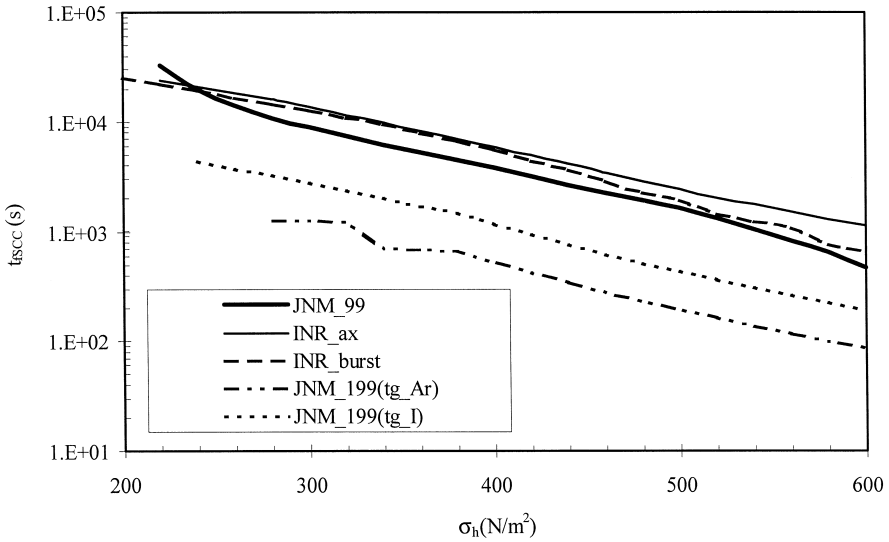

Fig. 2. The dependence of the SCC time to failure of the cladding, t_{fSCC}, on the macroscopic hoop stress, σ_h; $T = 614$ K; irradiated material.

3.2. The dependence of the stress threshold for transgranular crack propagation on the crystallographic orientation of the cracking plane and on the iodine fractional coverage

Following the calculations presented in Sections 2.2.1, 2.2.2 and 2.2.3, we could express the value of the threshold stress for the transgranular propagation of the crack for every given crystallographic plane and every chosen value of the fractional coverage. We considered the following constants in calculation: curvature radius at the crack tip, $\rho = 10^{-5}$ m; the distance corresponding to the restoring force vanishing, $\delta = 4 \times 10^{-9}$ m and the following values for the adjustable parameters of the model presented in Section 2.2.2; $\phi_0 = 8.24 \times 10^3$ m/s and $n = 1.5$.

We have calculated the dependence of the transgranular cracking threshold stress, $\sigma_{0,c+f}$, on the angle ω between the basal plane and the plane in which the breaking of the Zr–Zr bond takes place, in absence of iodine. We have considered

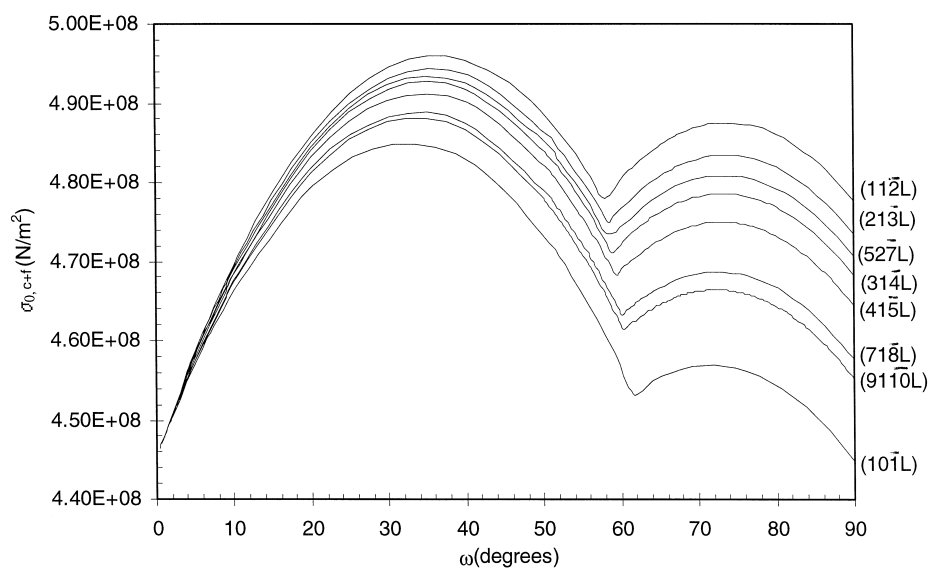

Fig. 3. The dependence of the threshold stress for transgranular cracking on the interplanar angle, ω, formed by the plane in which bond breaks with basal plane; $\theta = 0$.

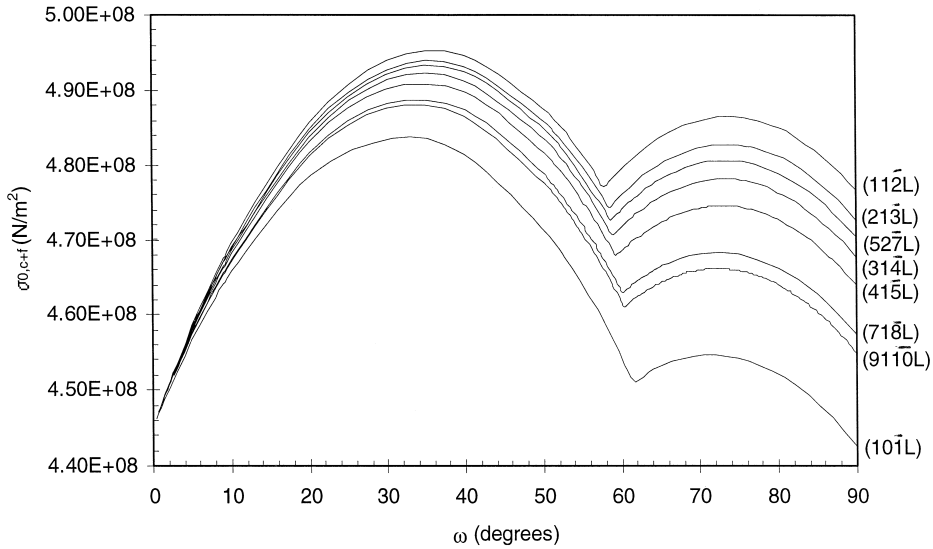

Fig. 4. The dependence of the threshold stress for transgranular cracking on the interplanar angle, ω, formed by the plane in which bond breaks with the basal plane; $\theta = 0.25$.

eight families of planes, such that [7] the corresponding $(hk10)$ planes were separated by approximately 5°. These families of planes were: $(11\bar{2}L)$, $(21\bar{3}L)$, $(52\bar{7}L)$, $(31\bar{4}L)$, $(41\bar{5}L)$, $(71\bar{8}L)$, $(91\bar{1}0L)$ and $(11\bar{2}L)$. The results are shown in Fig. 3. We performed the same calculations for other three values of the iodine fractional coverage: 0.25, 0.5 and 0.75 and the results are shown in Figs. 4–6, respectively. It is obvious that the stress threshold decreases with the increase of the fractional coverage. Figs. 3–6 show that the threshold stress variation with the crystallographic orientation of the plane is increased with increasing the iodine fractional coverage. For all the four θ values considered, the set of planes $(10\bar{1}L)$ minimized the threshold stress for transgranular propagation of the crack.

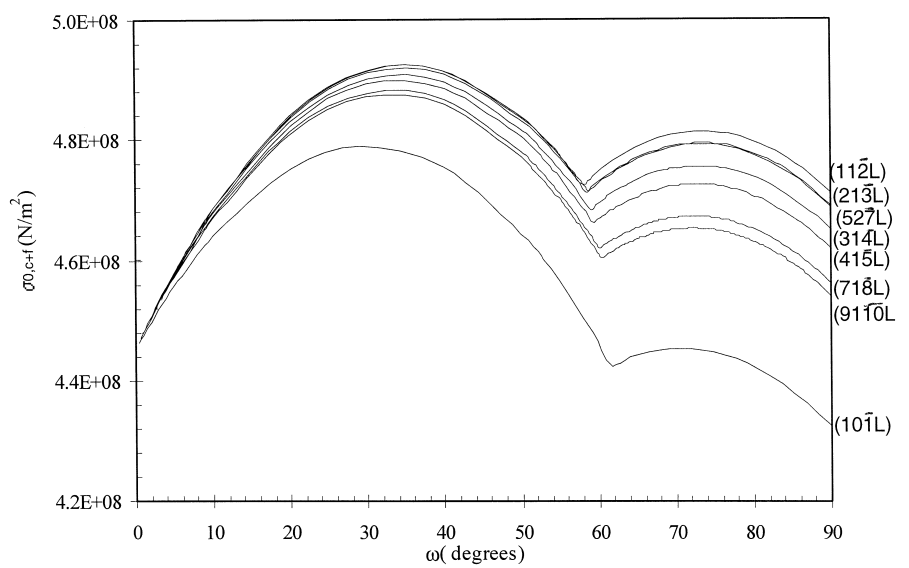

Fig. 5. The dependence of the threshold stress for transgranular cracking on the interplanar angle, ω, formed by the plane in which bond breaks with the basal plane; $\theta = 0.50$.

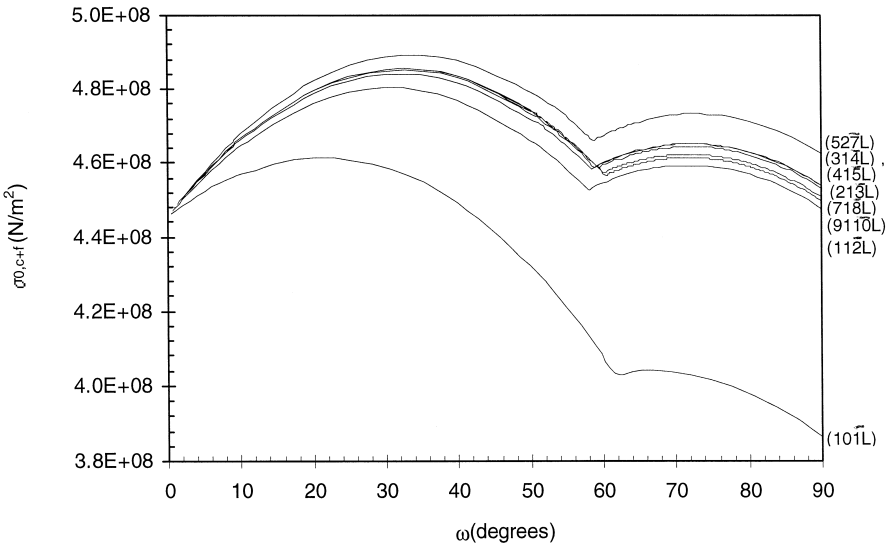

Fig. 6. The dependence of the threshold stress for transgranular cracking on the interplanar angle, ω, formed by the plane in which bond breaks with the basal plane; $\theta = 0.75$.

3.3. The SCC time to failure dependence on the crystallographic orientation of the cracking plane and on the iodine fractional coverage

We calculated dependence of the SCC time to failure, t_{fSCC}, on the orientation of the plane in which the breaking of the Zr–Zr bond takes place and on the iodine fractional coverage for two power ramps appearing at 135 MWh/kgU and 185 MWh/kgU. To do this, we used the overall model presented in Section 2.1 with the improvements described in Section 2.3.

In each case, we performed calculations for the family of planes $(10\bar{1}L)$ because as shown in Section 3.2, this family of planes is characterised by the lowest values the threshold stress for transgranular stress corrosion crack propagation and for the SCC time to failure. Previous calculations [27] have also shown that for this family of planes the surface energy, and the SCC time to failure have minimum values. To evaluate the actual value of the fractional coverage with ZrI_4 at the internal

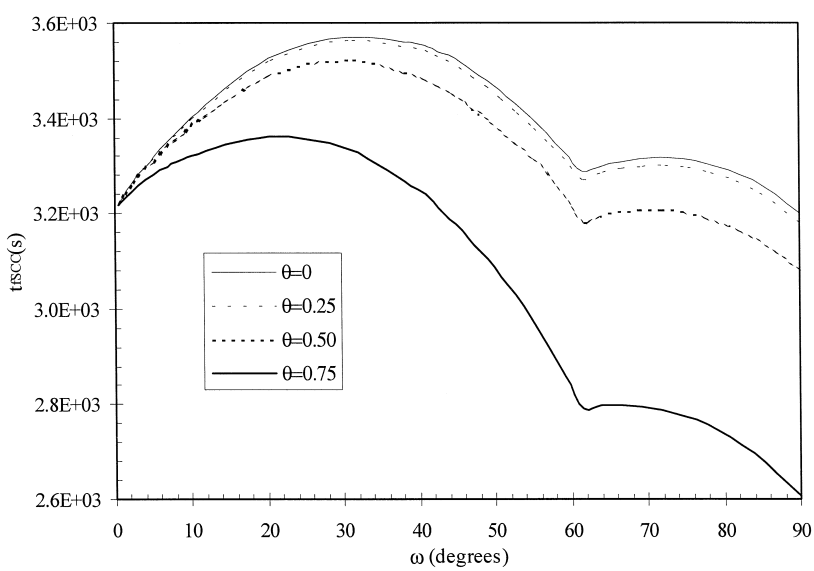

Fig. 7. The dependence of the time to SCC failure, t_{fSCC}, on the angle, ω, between the basal plane and the plane of the bond Zr–Zr which breaks and on the iodine fractional coverage for a power ramp at 135 MW h/kg U.

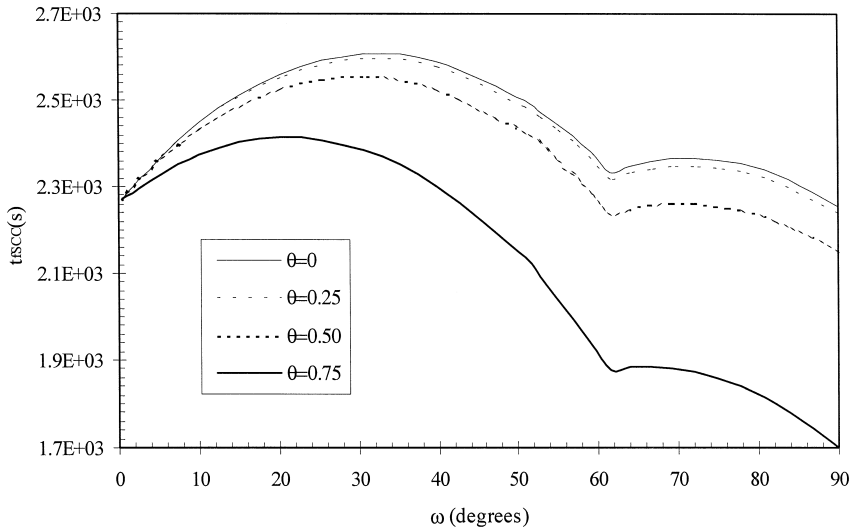

Fig. 8. The dependence of the time to SCC failure, t_{fSCC}, on the angle, ω, between the basal plane and the plane of the bond Zr–Zr which breaks and on the iodine fractional coverage for a power ramp at 185 MW h/kg U.

surface of the cladding detailed data on the iodine retention in the graphite by chemical reactions, absorption and adsorption are necessary but unfortunately we did not have such data but for the iodine adsorption [16]. We performed calculation for four different values of the fractional coverage with ZrI_4, 0, 0.25, 0.50 and 0.75 for each case we considered.

The calculated values of the times to failure have the order of magnitude of those observed in real power ramps. The results are presented in Figs. 7 and 8 and they show that the time to SCC failure decreases when the burnup at which the power ramp occurs increases and when the iodine fractional coverage increases. These results stress the capacity of our improved model to express quantitatively the dependence of the SCC time to failure on the iodine coverage and on the crystallographic orientation of the cracking plane.

4. Discussion and conclusions

We have developed a program to describe the evolution of the stress corrosion cracks in the fuel element cladding during power ramps and verified the possibility to apply the program for CANDU type fuel. Our goal was to express quantitatively the dependence of the SCC time to failure on the cracking plane orientation. We expressed the threshold stress for the transgranular crack propagation in terms of the surface energy using the Griffith criterion. Then, we took into account the dependence of the surface energy on the crystallographic orientation of the plane in which the breaking of the Zr–Zr bond takes place. It was thus possible to study the effect of the cracking plane orientation (perpendicular to the plane of the Zr–Zr bond being broken in the cracking process) and of the iodine fractional coverage on the value of the time to SCC failure.

Calculations have been made with the program and the values obtained for the times to failure were close to the actual ones. A strong dependence of the time to failure on the cracking plane orientation and on the iodine fractional coverage was observed.

It is possible to improve our method to evaluate the evolution of a stress corrosion crack in the fuel element cladding by quantifying the iodine adsorption in graphite based on available experimental data.

References

[1] M. Tayal, A. Ranger, N. Singhal, R. Mark, Evolution of the ELESTRES Code for Applications to Extended Burnups, AECL 9947, 1990.
[2] M. Tayal, E. Millen, R. Sejnoha, G. Vally, A Semi-Machanistic Approach to Calculate the Probability of Fuel Defects, AECL 10642, 1992.
[3] R.E. Williford, J. Nucl. Mater. 132 (1985) 52.
[4] E. Steinberg, M. Peehs, H. Stehle, J. Nucl. Mater. 118 (1983) 286.

[5] K. Konashi, M. Yamawaki, J. Nucl. Sci. Technol. 29 (1992) 1.
[6] R.E. Williford, Nucl. Eng. Design 78 (1984) 23.
[7] S.K. Hwang, H.T. Han, J. Nucl. Mater. 161 (1989) 175.
[8] W. Losch, Acta Metall. 27 (1979) 1885.
[9] R. Thomson, C. Hsieh, V. Rana, J. Appl. Phys. 42 (8) (1971) 3154.
[10] R. Thomson, J. Mater. Sci. 15 (1980) 1014.
[11] E.R. Fuller, R. Thomson, J. Mater. Sci. 15 (1980) 1027.
[12] T. Kubo, Y. Wakashima, K. Amano, M. Nagai, J. Nucl. Mater. 132 (1985) 1.
[13] A.K. Miller, H. Ocken, A. Tasooji, J. Nucl. Mater. 99 (1981) 254.
[14] L.O. Jernkvist, Nucl. Eng. Design 156 (1995) 393.
[15] P.K. Chan, K.G. Irving, J.R. Mitchel, The role of Zr_xI_yC compounds in minimizing SCC in fuel cladding, in: Proceedings of the 3rd International Conference on CANDU Fuel, Chalk River, Canada, October, 4–8, 1992.
[16] S. Mehedinteanu, Mechano-Chemical Model for the Fuel Element Cladding Failure at High Burnups, INR Internal Report 2709, 1989.
[17] W.J. Penn, R.K. Lo, J.C. Wood, Nucl. Technol. 34 (1977) 249.
[18] R.L. daSilva, -CAFE- probabilistic model for predicting CANDU fuel SCC power ramp failures, in: Proceedings of the 3rd International Conference on CANDU Fuel, Chalk River, Canada, Vol. 2, October, 4–8, 1992.
[19] E. Ciocan, E. Gheorghiu, G. Horhoianu, S. Ion, M. Tita, Model for CANDU fuel element sheath cracking through stress corrosion cracking mechanism, INR Internal Report, R.I. 4358, 1994.
[20] G. Lysell, D. Schrire, Fission Product Distribution at Different Power Levels, IAEA Meeting on Fuel Performance at High Burnup for Water Reactors, Studswik, Sweden, 1990, June 5–8, IWGEPT/36, pp. 132–139.
[21] B.R. Lawn, T.R. Wilshaw, Fracture of Brittle Solids, Cambridge University, 1975.
[22] A.S. Tetelman, A.J. McEvily Jr. (Eds.), Fracture of Structural Materials, Wiley, Chichester, 1967, pp. 38–85.
[23] M.L. Jokl, V. Vitek, C.J. McMahon, Acta Metall. 28 (1980) 1479.
[24] Y. Brechet, F. Louchet, Acta Metall. Mater. 41 (1993) 783.
[25] G. Horhoianu, D.R. Moscalu, V. Horhoianu, E. Ciocan, Evaluation of the irradiation effect on mechanical properties of the Zircaloy-4 fuel cladding irradiated in C5 device, INR Internal Report 2722, 1989.
[26] S.B. Goryachev, A.R. Gritsuk, P.F. Prasolov, J. Nucl. Mater. 199 (1992) 50.
[27] E. Ciocan, E. Gheorghiu, G.P. Papadopol, M. Tita, The role of the texture in the mechanism of the stress corrosion cracking: improvement of the SCC routine of the ELES code, INR Internal Report 5008, 1997.